	Additive manufacturing of forceps with continuous carbon fiber for virtual childbirth training	MECHANICAL
COLLABORATION	**Pablo Bordón, Rubén Paz, Mario Monzón, Ana González, Yamilet Rivero, Joshua García, Javier González, Alicia Pose, Cristina Soriano, Juan León, Juan Ruiz**	Others

ADDITIVE MANUFACTURING OF FORCEPS WITH CONTINUOUS CARBON FIBER FOR VIRTUAL CHILDBIRTH TRAINING

Pablo Bordón-Pérez1, Rubén Paz-Hernández1, Mario Monzón-Verona1, Ana González-Rodríguez1, Yamilet Rivero-López1, Joshua García-Montagut1, Javier Pascau González-Garzón2, Alicia Pose-Díez-de-la-Lastra2, Cristina Soriano-Ergui2, Juan-de-León Luis3 y Juan Ruiz Alzola1

1 Universidad de Las Palmas de Gran Canaria (España)

2 Universidad Carlos III de Madrid (España)

3 Universidad Complutense de Madrid (España)

DOI: https://dx.doi.org/10.52152/11091

1.- INTRODUCTION

Among the different types of delivery, instrumental vaginal delivery is one in which some type of tool is used to aid in the extraction of the fetus. In Europe, between 2014 and 2018, between 10 and 15% of deliveries were instrumentalized, with vaginal delivery with forceps (FAVD) being one of the most commonly used options worldwide [1]. This technique applies traction to the fetal head using generally two cephalic spoons or blades that self-couple thanks to their geometry and allow the fetus to be guided out of the birth canal during the uterine contraction phase [2,3]. In this way, delivery is facilitated in certain situations, being a recommended alternative to cesarean delivery (the World Health Organization recommends a cesarean section rate of less than 15% [4]).

Like any delivery procedure, FAVD has possible side effects and contraindications, although fewer than other instrumented processes such as vacuum systems [5]. In fact, in some medical fields, FAVD is declining due to a series of risks for both the mother and the fetus. Regarding the mother, it can cause severe vaginal tears that could even require surgery [6], higher rates of analgesia and perineal trauma [7], among others. As for the neonate, this technique can cause fetal facial injuries [8], deformities in the head or face of the fetus [9], neonatal complications, or even direct or postpartum fatal outcomes [10]. For those reasons, the use of forceps has led to a progressive rejection of their use, which is mainly associated with the lack of training and expertise since the technique requires a set of skills for safe and adequate execution [11]. In fact, the insecurity on the part of obstetricians can condition the use of the technique even in cases where it is the only resource [12]. The need to alleviate the decline in the use of forceps has promoted the development of FAVD training methods in recent years.

There are several FAVD training methods with anatomical simulators using phantoms or mannequins, usually made of polymeric materials, which include a pelvis with a fetus and a perineum with an anal sphincter [13,14]. Different studies have confirmed the need for this type of training prior to clinical experience in cases of childbirth assistance [15] significantly increasing the confidence of professionals [16]. Therefore, this type of training has become a crucial stage in the obstetric medical professional development that is allowing, albeit slowly, the increase in the use of the FAVD technique [17].

Electromagnetic tracking or navigation is a versatile technique in the medical field. It involves generating a low-intensity electromagnetic field in a designated working space. Microsensors placed in this field can be used to precisely locate the position and orientation of medical instruments in real-time without direct visual contact [18]. This application has been widely validated as a training method in a variety of anatomical examples [19]. However, the introduction of ferromagnetic materials in the work area significantly affects the dimensional precision, producing deviations of the system [19,20]. In the case of vaginal delivery, the electromagnetic tracking system has been shown to be a viable method for virtual training [22] although the use of stainless-steel commercial forceps is not feasible due interference issues. The utilization of nylon and aluminum powder through additive manufacturing (AM) technologies has partially solved this problem. However, deformations in the forceps during training result in dimensional distortions that require improvement [23], as they can alter the virtual positioning and the perceived rigidity of the instrument by obstetricians.

AM has greatly expanded possibilities in the medical field, with multiple growing areas such as manufacturing with biomaterials, biotissues, or biomodels for training [24]. AM has enormous potential in relation to surgical instruments [25], such as the improvement of molar forceps. [26]. Even in relation to anatomical models, some authors claim that more than 87% are made with AM [5], being used in preoperative plans, training systems, or medical research.

Forceps for vaginal delivery have been the subject of numerous studies, from the interaction of forceps with the fetal head [26] to the analysis of excessive deformation due to incorrect placement of the blades [27], or their validation through training simulators during obstetric manipulation as a teaching tool [28].

ISSN: 0012-7361 eISSN: 1989-1490 / DYNA Vol.99 N.4 DOI: https://doi.org/10.52152/11017

Advanced material extrusion (MEX) technologies, such as Mark Two from Markforged, Inc., now enable the integration of continuous fibers (rather than just short fibers), embedded continuously, layer by layer, in the polymer matrix, significantly improving the continuity of reinforcement. This capability allows to produce high-strength models without electromagnetic incompatibility, using materials like nylon reinforced with carbon microfibers (Onyx).

This work presents the development of a non-metallic forceps, designed for vaginal delivery training through electromagnetic positioning guidance, materialized through additive manufacturing by material extrusion (MEX) using nylon reinforced with both microfiber and high-rigidity continuous carbon fiber.

2.- MATERIALS AND METHODS

2.1.- MATERIALS AND MANUFACTURING METHODS

For preliminary tests, polylactic acid (PLA) filament from Smartfil was utilized with the Anycubic i3 Mega S printer (Hongkong Anycubic Technology Co., Ltd.) with a 0.6 mm nozzle, 0.2 mm layer height, 210 ºC printing temperature, 60ºC bed temperature, 50 mm/s printing speed, and 100% rectilinear infill.

As the definitive material for obtaining the training forceps, the commercial filament Onyx was used (nylon internally reinforced with microfibers of carbon -Markforged, Inc., USA-). Additional reinforcement was provided by CF-BA-50 continuous carbon fiber from the same manufacturer. The combination of both materials generates composite parts henceforth referred to as Onyx CCF. These materials were used in the Mark Two MEX printer from Markforged, Inc., which has a 1.75 mm filament extruder and a continuous fiber feeder with a polymer layer embedding system. With the integrated Eiger software, the orientations and layers of continuous carbon fiber reinforcement were established with a 0.4 mm nozzle, 0.125 mm layer height, maximum printing temperature of 300 ºC, and solid infill were used.

Finally, a two-component epoxy resin, 43249 Resina 3D from Industrias Químicas Eurotex S.L.U., was used as the adhesive to join the different parts of the forceps. The flowchart of the manufacturing processes and general methodology is summarized in Figure S1.

2.2.- JOINT MODELING PROCESSES

Due to the dimensions of the commercial forceps model (414 mm in length) (Figure S2), which surpass the printing capacity of the Mark Two technology (320 mm in length), SolidWorks 2016 software (Dassault Systèmes Corporation) was utilized to design the forceps partition, divided in its intermediate zone, between the handle and the cephalic spoon. Finally, a mechanical union by shape was selected, using a hollow spigot coupling and dovetail geometry (Figure 1). To enhance bonding, both the spigot and the hollow were given a longitudinally toothed surface and epoxy adhesive was applied.

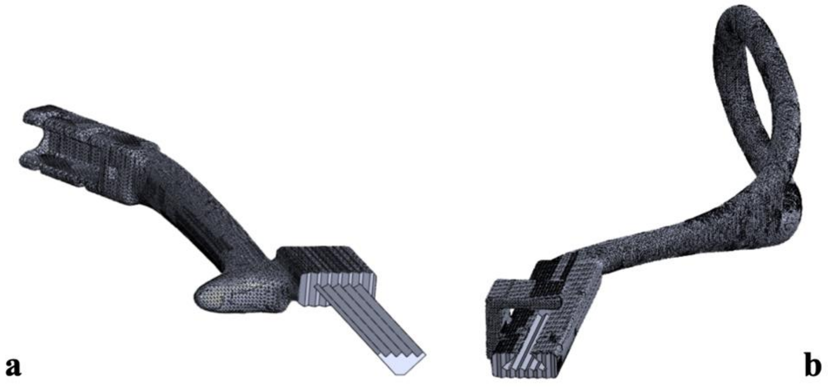

Figure 1: Forceps partition design using a) tang in handle and b) hollow in cephalic spoon.

On the other hand, to obtain the best mechanical performance of the joints, 4 joint variants were modeled by combining the assembly clearance (0.25 and 0.35 mm) and the front surfaces of the joint (smooth or toothed front contact) (Figure S3).

2.3.- MECHANICAL BEHAVIOR SIMULATIONS

To analyze the mechanical behavior of the forceps during virtual training, mechanical simulations were carried out using Abaqus CAE software (Dassault Systèmes Simulia Corp). Maximum displacement under operating loads and the displacement of the midpoint of

ISSN: 0012-7361 eISSN: 1989-1490 / DYNA Vol.99 N.4 DOI: https://doi.org/10.52152/11017

the forceps handle have been analyzed as a representative measure of perceived handle displacement during use. To establish an adequate comparative framework, a commercial stainless-steel forceps was initially simulated as an initial reference.

Considering materials for electromagnetic interference-free forceps, a standard aluminum forceps, suitable for casting, or additive manufacturing, was simulated due to its non-ferrous properties and high elastic limit. Additionally, three materials optimized for additive manufacturing were explored: polyamide and aluminum powder (called alumide and of comparative interest for having been used in the manufacture of forceps for virtual training [22]), polyamide reinforced with carbon microfiber (Onyx), and Onyx with an additional continuous carbon fiber reinforcement (Onyx CCF).

The simulations of the forceps were carried out using a simplified modeling approach, using one of the two instrument blades, since the mechanical operation of both parts of the forceps is practically symmetrical. As the first boundary condition, a fixed support was applied to the internal surfaces of the cephalic spoon, reproducing the rigid grip of the fetal head (Figure 2a). Simultaneously, a transverse direction movement restriction was applied to the forceps (without displacement in the x-axis) on the vertices where the contact between the blades begins during the forceps closing process. This condition reproduces the pivoting of both forceps' blades between them. (Figure 2b). Finally, equivalent loads produced during the FAVD technique were applied, corresponding to a force of 100 N applied to the handle and in the direction of the forceps' closure, and a traction force of 200 N on the upper part of the handle and in the direction of the fetus' extraction (Figure 2c). These forces were applied according to empirical data obtained by different authors [27,28].

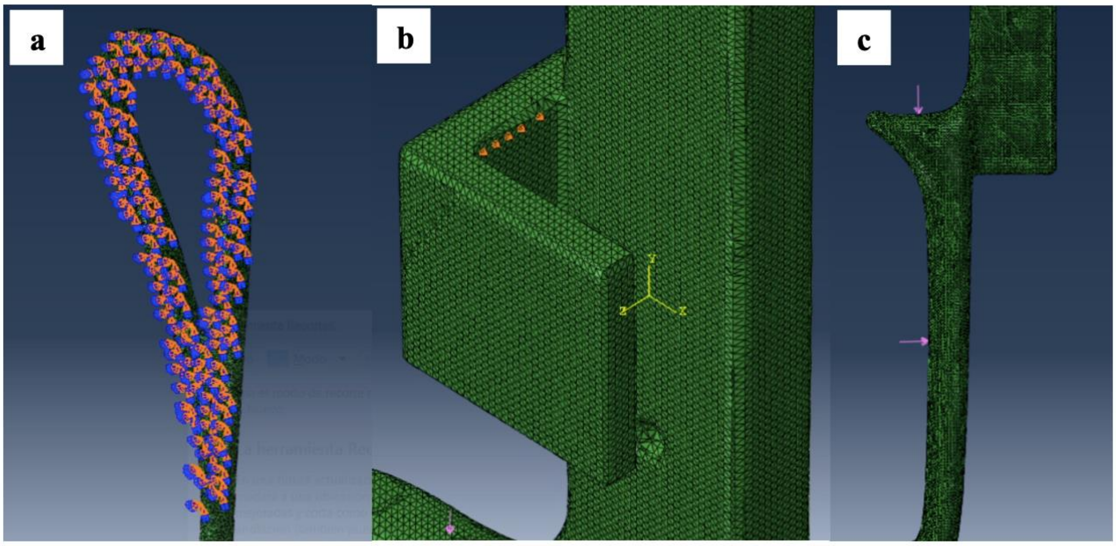

Figure 2: Boundary conditions: a) embedment in the cephalic spoon, b) movement restriction in x in the forceps pivot area and c) closing and extraction forces of the forceps.

The mechanical properties for the different materials used are shown in Table 1.

Material	Elastic modulus (GPa)	Strength strain (MPa)	Poisson coefficient
Stainless steel [29]	193.0	215	0.30
Aluminum [30,31]	69.0	95	0.33
Alumide [32]	3.8	48	0.41
Onyx [33,34]	2.4	37	0.42
Onyx CCF	13.7[1]	443[1,2]	0.35 [35]

[1] Data obtained from empirical tests according to section 0 y 0. [2] Breaking stress is used due to the fracture without plastic deformation in the tests.

Table 1: Mechanical properties of materials.

2.4.- MECHANICAL CHARACTERIZATION

ISSN: 0012-7361 eISSN: 1989-1490 / DYNA Vol.99 N.4 DOI: https://doi.org/10.52152/11017

The different mechanical joints designed to assemble the two parts of the forceps blade (cephalic spoon and handle) were mechanically analyzed through tensile tests. 3 replicas of each design were manufactured and tested, made in PLA. For this, an LY-1065 test machine (Dongguan Liyi Test Equipment Co. Ltd., Dongguan, China) was used, with an average distance between jaws of 55 mm and a loading speed of 1 mm/min until breakage.

To obtain the mechanical properties of Onyx CCF, 3 specimens were flex tested according to the ISO 178:2019 standard. The specimens were manufactured as per section 2.1 with dimensions of 10 mm in width, 4 mm in thickness, and 80 mm in length. The same test equipment described above was used, with a support distance of 64 mm and a loading speed of 10 mm/min until breakage.

2.5.- VALIDATION IN TRAINING SYSTEM THROUGH ELECTROMAGNETIC GUIDANCE

The basic electromagnetic compatibility validation of the forceps with the guidance system was carried out using a virtual childbirth training system (Figure S4) composed of 2 6DOF sensors for mounting on the end of the forceps, a 3D Guidance trakSTAR electromagnetic positioning system (Northern Digital Inc.), a PROMPT Flex - Advanced Light Skin Tone birthing training mannequin (Limbs & Things LTD), and the open-source software 3D Slicer (BWH and 3D Slicer contributors).

3.- RESULTS AND DISCUSSIONS

3.1.- MECHANICAL TESTS

The tensile tests carried out on the different joint configurations that were designed (Figure 3) show average values within a similar magnitude range and low dispersion of the results (Table 2). All designs far exceed the tensile loads that would be applied during the use of the forceps, with a material (PLA) of lower performance than the Onyx CCF, confirming the suitability of any of the designed joint systems. The design with 0.25 mm of clearance and front groove was selected because it had the highest breaking stress, even if there is no statistical significance.

Configuration	Breaking strain (N)
0.25 mm without front slot	819.97 ± 28.24
0.35 mm without front slot	1085.50 ± 65.76
0.25 mm with front slot	1098.50 ± 78.49
0.35 mm with front slot	984.50 ± 79.90

Table 2: Results of the tensile tests of joints.

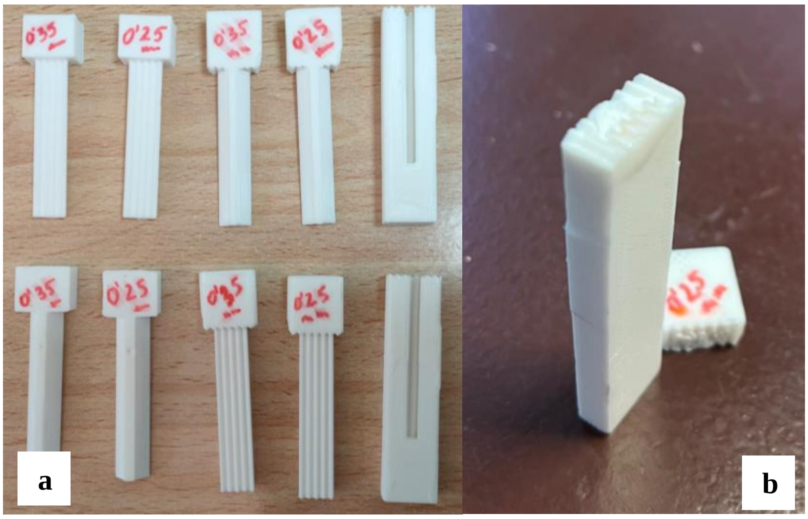

Figure 3: a) Sample of joint specimens and b) sample after breakage test.

In relation to the flexural tests carried out on the Onyx CCF specimens (Table 3), the results showed a high flexural breaking stress, averaging over 450 MPa, with no defined elastic limit due to the high stiffness. The incorporation of continuous carbon fiber significantly increased the properties of the composite.

ISSN: 0012-7361 eISSN: 1989-1490 / DYNA Vol.99 N.4 DOI: https://doi.org/10.52152/11017

The forceps modeling with Onyx CCF was simplified considering an isotropic behavior based on these results.

Specimens	Elastic modulus (GPa)	Breaking strain (MPa)
1	15.46	467.89
2	13.33	457.18
3	12.38	433.83
Average and standard deviation	13.72 ± 1.58	452.97 ± 17.42

Table 3: Result of flexural tests of Onyx CCF specimens.

3.2.- FORCEPS MECHANICAL SIMULATION

The results obtained in the mechanical simulations of the forceps are summarized in Table 4.

Material	Maximum von Mises stress (MPa)	Maximum displacement (mm)	Mid-handle displacement (mm)
Stainless steel	84.50	0.07	0.04
Aluminum	81.48	0.19	0.09
Alumide	71.22	3.51	1.79
Onyx	69.48	5.54	2.82
Onyx CCF	79.30	0.98	0.50

Table 4: Mechanical simulation results of the forceps according to material.

The maximum stresses (Figure 4) would cause significant plastic deformations and fractures in forceps made of alumide and standard Onyx. In the case of stainless steel, aluminum, and Onyx CCF, only transient elastic deformations would be produced. It is worth noting that these stress concentrations also derived from the modeling of the boundary conditions of the pivot, which has been modeled using points in the contact area between the two blades of the forceps.

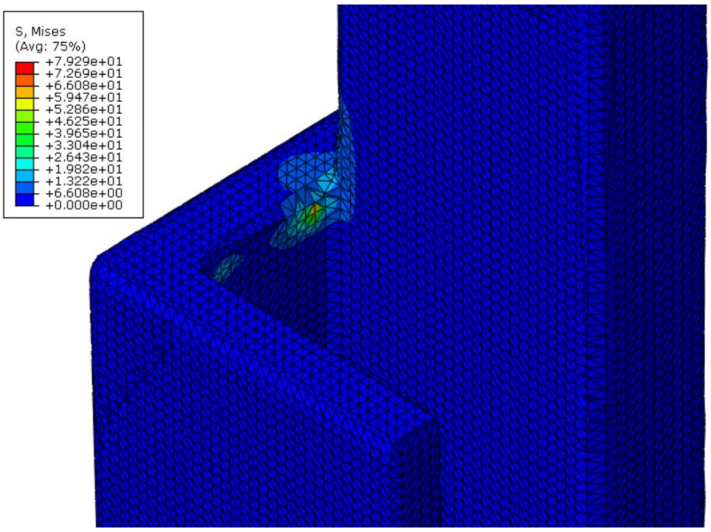

Figure 4: Maximum von Mises stresses in the pivot area of the forceps.

The applied forces do not produce significant stresses that would compromise the Onyx CCF model, generating minor stresses in the external area, located between the cephalic spoon and the handle, and negligible stresses in the partition area of the forceps.

Regarding the maximum displacements, these occur at the end of the handle, where the electromagnetic positioning sensors are located. The maximum displacement of the stainless-steel commercial model, is only 0.07 mm, indicating a high mechanical stiffness. The alumide and Onyx models reach considerable maximum displacements, of 3.51 and 5.54 mm respectively, while the incorporation of continuous carbon fiber in the Onyx matrix allows for a substantial increase in the stiffness, reducing the maximum displacement to

ISSN: 0012-7361 eISSN: 1989-1490 / DYNA Vol.99 N.4 DOI: https://doi.org/10.52152/11017

0.98 mm (82% lower than standard Onyx). The model made using conventional aluminum, however, would achieve maximum displacements of 0.19 mm, closer to the reference model.

Additionally, the displacements of the midpoint of the forceps handle have been calculated, considering that such displacement might more accurately represent the displacement perceived during FAVD training. Under this assumption, the displacements decrease to values close to 50% compared to those at the end of the handle, bringing the displacements of the aluminum model closer to the commercial model, and reducing the differences between the Onyx CCF and aluminum models to values around 0.4 mm (last column of Table 4). The displacement values for Onyx CCF, in both cases, of 0.98 mm maximum value and 0.5 mm at the midpoint of the handle, might be compatible with the proper development of FAVD training, given the difference compared to the simulated commercial model.

3.3.- RESULTS OF THE ORIENTATION ANALYSIS AND MANUFACTURING OF THE ONYX CCF FORCEPS

The effective orientation of the continuous deposited carbon fiber fundamentally depends on the orientation angle, the fiber pattern type, the alignment of the piece with the working axes of the printer, and the tilt of the piece in the vertical printing axis.

Different configurations of both piece orientation and fiber insertion patterns were analyzed. Regarding the horizontal orientation of the piece, this variable had minor effects since the fiber is largely oriented in the main direction of the piece when considering a combined pattern of continuous fiber fill, both isotropic and concentric. This configuration allows the fiber to align with the contour of the piece throughout its variable geometry from concentric continuous fiber rings (concentric pattern) to the edges of the piece (Figure 5 a), benefiting the bending behavior. Longitudinally, the internal fill with a 0º direction (isotropic pattern) aligns in the main direction of the forceps (also horizontally oriented at 0º), benefiting the overall tensile behavior (Figure 5 b).

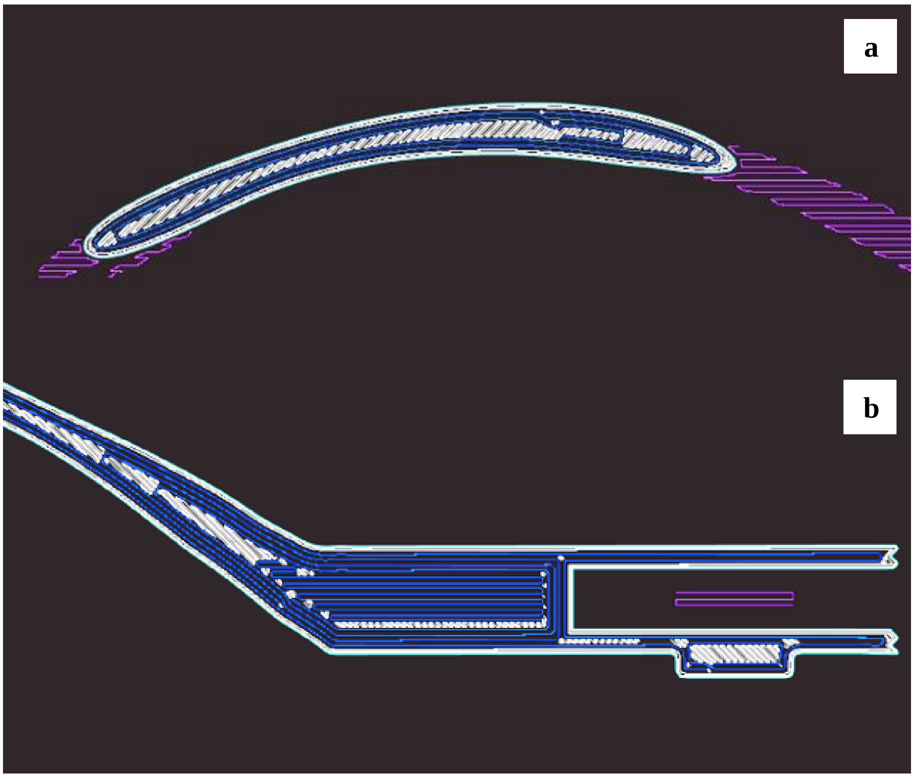

Figure 5: Sections with continuous reinforcement fiber (blue lines) configured in the Eiger software. a) Concentric perimeter of the cephalic blade and b) 0º isotropic fill at the base of the cephalic blade.

In relation to vertical orientation, different orientation analyses were carried out since it significantly influences the inclination of the layers that generate the piece and modifies the surfaces available for continuous fiber deposition. Given that this technology requires

ISSN: 0012-7361 eISSN: 1989-1490 / DYNA Vol.99 N.4 DOI: https://doi.org/10.52152/11017

a minimum fiber length of 45 mm for deposition, achieving complete reinforcement across the entire geometry is usually not feasible. Therefore, it becomes necessary to seek the most effective combination of reinforcements.

After multiple configurations, the best orientation corresponds to the one shown in Figure 6, with a solid fill pattern, concentric fiber of 4 rings, 0º isotropic fiber, and handle alignment with the horizontal printing plane as vertical orientation. This configuration produces one of the highest ratios of continuous fiber (Table 5), the most fiber introduction in the area of maximum stresses (coupling and pivoting area of the forceps blades), and the fewest piece sections without continuous fiber (mid-end of the cephalic blade).

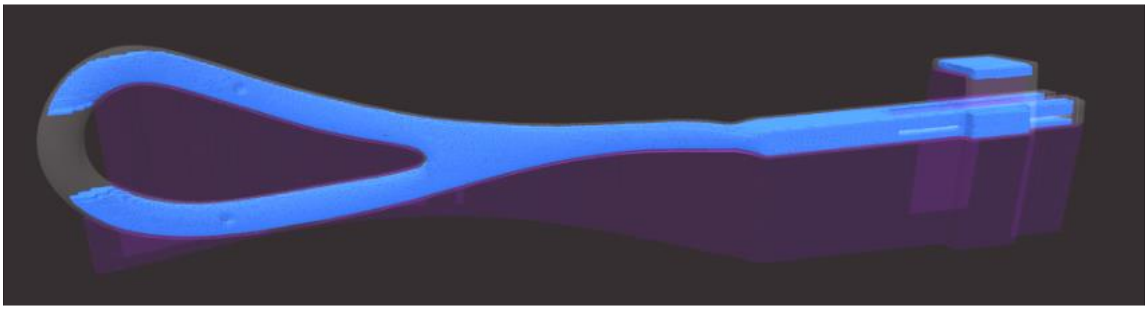

Figure 6: Layer segmentation in Eiger software with areas of continuous fiber reinforcement (blue areas) and areas without continuous fiber reinforcement (gray areas).

Part	Onyx (cm^3)	Carbon fiber (cm^3)
Left cephalic blade	69.96	17.39
Left handle	16.99	4.80
Right cephalic blade	61.90	15.09
Right handle	13.86	3.12

Table 5: Estimated material volume with Eiger software in the selected orientation.

3.4.- VALIDATION IN THE FAVD TRAINING SYSTEM

The result of the manufacturing and assembly process of the different parts of the forceps is shown in Figure 7. The total manufacturing cost amounted to 183.28 USD, corresponding solely to material costs, with the four parts taking a total of 60 hours to complete the printing.

ISSN: 0012-7361 eISSN: 1989-1490 / DYNA Vol.99 N.4 DOI: https://doi.org/10.52152/11017

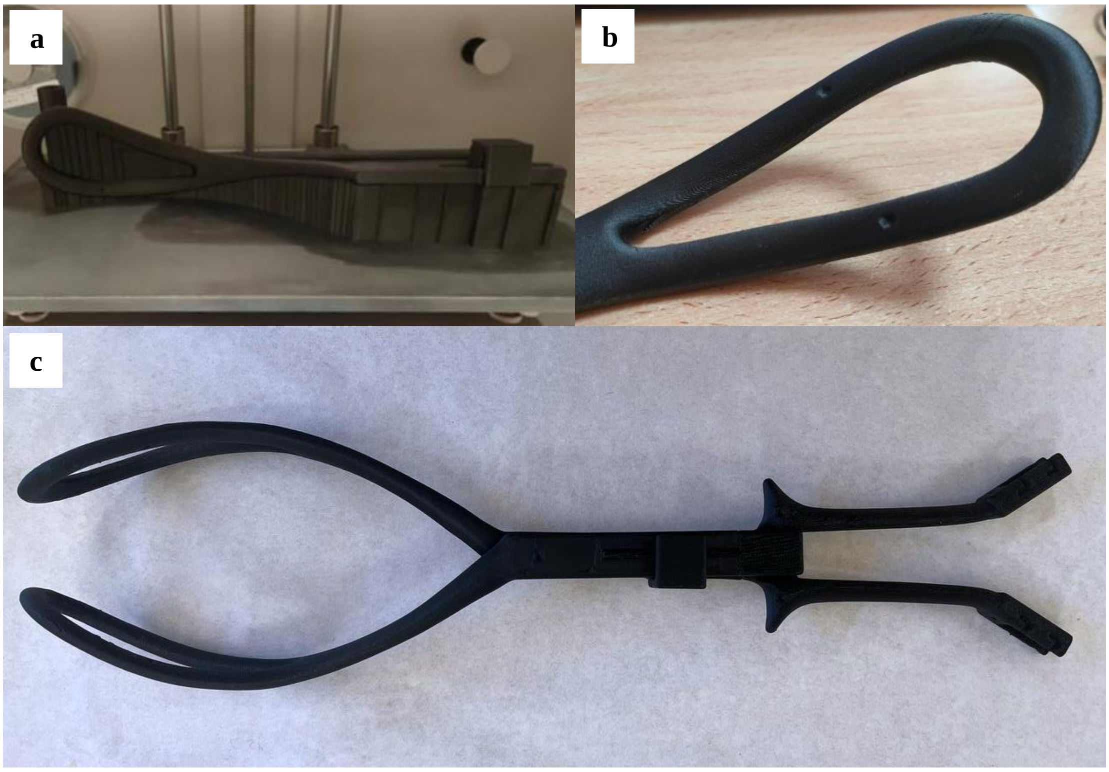

Figure 7: Forceps made in Onyx CCF: a) forceps blade on the print bed, b) detail of the cephalic blade's surface finish, and c) fully assembled forceps with adhesive.

The forceps validation in the virtual navigation system using electromagnetic positioning (Figure 8 b) was entirely satisfactory. The sensors aligned as expected, and no displacements occurred during use. Regarding the system's electromagnetic field, during the tests, the values for electromagnetic interference were null, confirming the full compatibility of the forceps, made of Onyx CCF, with these types of positioning systems.

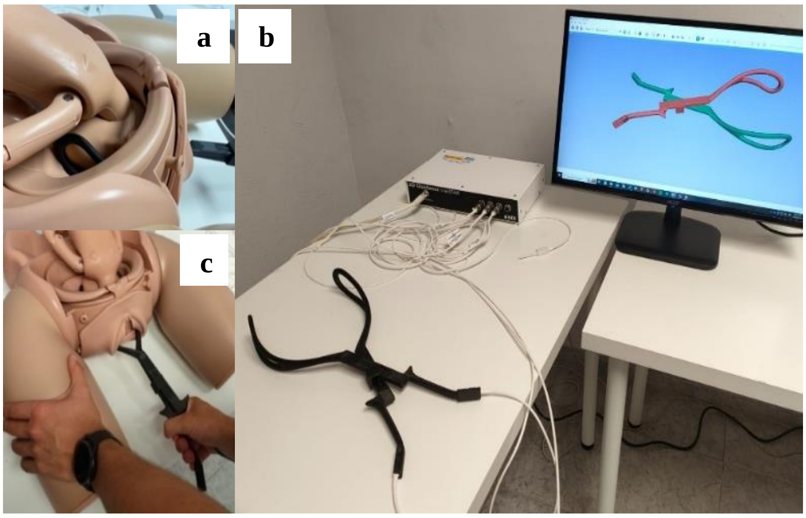

Figure 8: Validation of the forceps in the virtual training system: a) coupling of the forceps with the fetal mannequin, b) forceps mounted in the electromagnetic positioning system, and c) basic qualitative test of the forceps' positioning and closure.

ISSN: 0012-7361 eISSN: 1989-1490 / DYNA Vol.99 N.4 DOI: https://doi.org/10.52152/11017

The qualitative results from the tests with the training mannequin showed deformations consistent with the results obtained in the simulations, with a high stiffness of the manufactured model observed and displacements only noticeable with a significant increase in the forces applied to the forceps. Additionally, a proper grip and positioning with the fetus's head were perceived (Figure 8 a), as well as a suitable coupling of the blades during the forceps closing process (Figure 8 c).

4.- CONCLUSIONS

This research presents the results of the mechanical simulation, manufacturing, and validation of a vaginal birth forceps, specifically manufactured using 3D printing (MEX) with nylon doubly reinforced with short and continuous carbon fiber (Onyx CCF) for its use in FAVD training using virtual navigation systems by electromagnetic positioning.

The partition of the forceps blades allows obtaining forceps with mechanical capabilities much higher than those required during FAVD training practices. These reinforced Onyx forceps, with higher rates of continuous carbon fiber incorporation, exhibit mechanical stiffness quite close to models made of aluminum or stainless steel, with a deformation difference of less than 0.5 mm in the middle of the handle. Real-life forceps usage tests showed no deformations in the area of the cephalic blades or in the joints of the different parts.

Onyx CCF material showed no interference with the electromagnetic field. Therefore, the proposal of Onyx material reinforced with continuous carbon fiber stands as an alternative solution to other materials and technologies used in the manufacturing of forceps for FAVD training. For future medical training, conducting additional real tests to analyze deformations and their impact on perception is desirable. Real-time monitoring trials with the electromagnetic positioning system and additional sensors at critical deformation points would help in this analysis.

Finally, it is worth noting that the use of additive manufacturing with materials like Onyx CCF allows the production of many other surgical training instruments, compatible with electromagnetic positioning systems, where high stiffness (or even high dimensional accuracy) is required without resorting to higher-cost technologies such as the fusion of non-ferromagnetic metallic powder beds.

ACKNOWLEDGEMENTS

This work has been co-funded by the Macbioidi2 project (MAC2/1.1b/352, European Regional Development Fund INTERREG, MAC territorial cooperation program).

REFERENCES

[1] Lebraud, M.; Loussert, L.; Griffier, R.; Gauthier, T.; Parant, O.; Guerby, P. Maternal and Neonatal Morbidity after Forceps or Spatulas-Assisted Delivery in Preterm Birth. European Journal of Obstetrics and Gynecology and Reproductive Biology 2022, 271, 128–131, doi:10.1016/j.ejogrb.2022.02.007.
[2] Forceps Delivery Available online: https://www1.cgmh.org.tw/intr/intr5/c6700/OBGYN/f/web/Forcep Delivery/index.htm (accessed on 16 March 2023).
[3] What Is a Gentle C-Section? Birth Plan, Options, and More Available online: https://www.healthline.com/health/pregnancy/gentle-c-section#bottom-line (accessed on 16 March 2023).
[4] Appropriate Technology for Birth. Lancet 1985, 2, doi:10.1016/s0140-6736(85)90673-7.
[5] Delivery, I.V. Guideline No. 26. 2005, 1–13.
[6] Parto Con Fórceps: MedlinePlus Enciclopedia Médica Available online: https://medlineplus.gov/spanish/ency/patientinstructions/000509.htm (accessed on 5 May 2023).
[7] Hernández-Hernández, D.; Laura Ramírez-Montiel, M.; Pichardo-Cuevas, M.; Moreno-Sánchez, J.A.; Jaimes Rodríguez, M.; Agustín Contreras-Carreto, N. Complicaciones Maternas y Neonatales Secundarias a Parto Vaginal Instrumentado Con Fórceps ARTÍCULO ORIGINAL. Rev Invest Med Sur Mex, Abril-Junio 2012, 19, 52–55.
[8] Moreno-Santillán, A.; González-Barreto, R.A. Forceps versus Vacuum. Comparison of Maternal and Fetal Success Rates and Complications. Ginecol Obstet Mex 2021, 89, 357–363, doi:10.24245/gom.v89i5.4951.
[9] Muraca, G.M.; Boutin, A.; Razaz, N.; Lisonkova, S.; John, S.; Ting, J.Y.; Scott, H.; Kramer, M.S.; Joseph, K.S. Maternal and Neonatal Trauma Following Operative Vaginal Delivery. CMAJ. Canadian Medical Association Journal 2022, 194, E1–E12, doi:10.1503/cmaj.210841.
[10] Ferraz, A.; Nunes, F.; Resende, C.; Almeida, M.C.; Taborda, A. Short-Term Neonatal Outcomes of Vacuum-Assisted Delivery. A Case-Control Study. An Pediatr (Engl Ed) 2019, 91, 378–385, doi:10.1016/j.anpedi.2018.11.016.
[11] Xin, S.; Wang, Z.; Lai, H.; Liu, L.; Shen, T.; Xu, F.; Zeng, X.; Zheng, J. Clinical Effects of Form-Based Management of Forceps Delivery under Intelligent Medical Model. J Healthc Eng 2021, 2021, doi:10.1155/2021/9947255.
[12] Nolens, B.; Capelle, M.; van Roosmalen, J.; Mola, G.; Byamugisha, J.; Lule, J.; Faye, A.; van den Akker, T. Use of Assisted Vaginal Birth to Reduce Unnecessary Caesarean Sections and Improve Maternal and Perinatal Outcomes. Lancet Glob Health 2019, 7, e408–e409, doi:10.1016/S2214-109X(19)30043-9.
[13] Dupuis, O.; Moreau, R.; Pham, M.T.; Redarce, T. Assessment of Forceps Blade Orientations during Their Placement Using an Instrumented Childbirth Simulator. BJOG 2009, 116, 327–333, doi:10.1111/j.1471-0528.2008.02004.x.
[14] Macedonia, C.R.; Gherman, R.B.; Satin, A.J. Simulation Laboratories for Training in Obstetrics and Gynecology. Obstetrics and Gynecology 2003, 102, 388–392, doi:10.1016/S0029-7844(03)00483-6.
[15] Murphy, D.J.; Liebling, R.E.; Verity, L.; Swingler, R.; Patel, R. Early Maternal and Neonatal Morbidity Associated with Operative Delivery in Second Stage of Labour: A Cohort Study. Lancet 2001, 358, 1203–1207, doi:10.1016/S0140-6736(01)06341-3.
[16] Crosby, D.A.; Sarangapani, A.; Simpson, A.; Windrim, R.; Satkunaratnam, A.; Higgins, M.F. An International Assessment of Trainee Experience, Confidence, and Comfort in Operative Vaginal Delivery. Ir J Med Sci 2017, 186, 715–721, doi:10.1007/s11845-017-1593-0.

[17] Hotton, E.; O'Brien, S.; Draycott, T.J. Skills Training for Operative Vaginal Birth. Best Pract Res Clin Obstet Gynaecol 2019, 56, 11–22, doi:10.1016/j.bpobgyn.2018.10.001.
[18] Electromagnetic Tracking Systems - NDI Available online: https://www.ndigital.com/electromagnetic-tracking-technology/ (accessed on 2 June 2023).
[19] Schwein, A.; Kramer, B.; Chinnadurai, P.; Walker, S.; O'Malley, M.; Lumsden, A.; Bismuth, J. Flexible Robotics with Electromagnetic Tracking Improves Safety and Efficiency during in Vitro Endovascular Navigation. J Vasc Surg 2017, 65, 530–537, doi:10.1016/j.jvs.2016.01.045.
[20] Soteriou, E.; Grauvogel, J.; Laszig, R.; Grauvogel, T.D. Prospects and Limitations of Different Registration Modalities in Electromagnetic ENT Navigation. European Archives of Oto-Rhino-Laryngology 2016, 273, 3979–3986, doi:10.1007/s00405-016-4063-9.
[21] Morchi, L.; Tognarelli, S.; Menciassi, A. A Novel Childbirth Simulator for Real-Time Monitoring of Fetal Head During the Active Phase of the Labor. IEEE Trans Med Robot Bionics 2022, 4, 720–728, doi:10.1109/TMRB.2022.3191494.
[22] García-Sevilla, M.; De León-Luis, J.; Moreta-Martínez, R.; García-Mato, D.; Pérez-Mañanes, R.; Calvo-Haro, J.; Pascau, J. Performance Evaluation to Improve Training in Forceps-Assisted Delivery. Lecture Notes in Computer Science (including subseries Lecture Notes in Artificial Intelligence and Lecture Notes in Bioinformatics) 2018, 11041 LNCS, 69–77, doi:10.1007/978-3-030-01201-4_9.
[23] Zadpoor, A.A.; Malda, J. Additive Manufacturing of Biomaterials, Tissues, and Organs. Ann Biomed Eng 2017, 45, 1–11, doi:10.1007/s10439-016-1719-y.
[24] Chang, T.B.; Bhatia, S.K. Assessment of 3D Printing for Surgical Instrument Manufacturing. Proceedings of the 8th World Congress on New Technologies 2022, 1–7, doi:10.11159/icbb22.007.
[25] Told, R.; Marada, G.; Rendeki, S.; Pentek, A.; Nagy, B.; Molnar, F.J.; Maroti, P. Manufacturing a First Upper Molar Dental Forceps Using Continuous Fiber Reinforcement (Cfr) Additive Manufacturing Technology with Carbon-Reinforced Polyamide. Polymers (Basel) 2021, 13, doi:10.3390/polym13162647.
[26] Lapeer, R.J. Contact Mechanics Simulation for Obstetric Forceps Delivery. 2004.
[27] Lapeer, R.; Audinis, V.; Gerikhanov, Z.; Dupuis, O. A Computer-Based Simulation of Obstetric Forceps Placement. Med Image Comput Comput Assist Interv 2014, 17, 57–64.
[28] Rodr, E.; Kypson, A.P.; Moten, S.C.; Nifong, L.W.; Jr, W.R.C. Robotic Mitral Surgery at East Carolina University: International Journal 2006, 211–215, doi:10.1002/rcs.
[29] ASM Material Data Sheet Available online: https://asm.matweb.com/search/SpecificMaterial.asp?bassnum=mq304a (accessed on 9 June 2023).
[30] Young's Modulus, Tensile Strength and Yield Strength Values for Some Materials Available online: https://www.engineeringtoolbox.com/young-modulus-d_417.html (accessed on 16 March 2023).
[31] Poisson's Ratio Available online: https://www.engineeringtoolbox.com/poissons-ratio-d_1224.html (accessed on 26 May 2023).
[32] Polyamide 6 | Designerdata Available online: https://designerdata.nl/materials/plastics/thermo-plastics/polyamide-6 (accessed on 16 March 2023).
[33] Polyamide (PA12) for Industrial 3D Printing | EOS Available online: https://www.eos.info/en/3d-printing-materials/plastic/polyamide-pa-12-alumide (accessed on 9 June 2023).
[34] Lammens, N.; De Baere, I.; Van Paepegem, W. On the Orthotropic Elasto-Plastic Material Response of Additively Manufactured Polyamide 12. 7th bi-annual international conference of Polymers \& moulds innovations (PMI 2016) 2016, 2.
[35] Parmiggiani, A.; Prato, M.; Pizzorni, M. Effect of the Fiber Orientation on the Tensile and Flexural Behavior of Continuous Carbon Fiber Composites Made via Fused Filament Fabrication. International Journal of Advanced Manufacturing Technology 2021, 114, 2085–2101, doi:10.1007/s00170-021-06997-5.

SUPPLEMENTARY MATERIAL

http://www.revistadyna.com/documentos/pdfs/_adic/11091-1_en.pdf

ISSN: 0012-7361 eISSN: 1989-1490 / DYNA Vol.99 N.4 DOI: https://doi.org/10.52152/11017